

Supplementary Information

ReGaGe₂: Intermetallic Compound with Semiconducting Properties and Localized Bonding

Maxim S. Likhanov,^a Roman A. Khalaniya,^a Valeriy Yu. Verchenko,^{ab} Andrei A. Gippius,^{cd} Sergei V. Zhurenko,^{cd} Alexey V. Tkachev,^d Dina I. Fazlizhanova,^c Alexey N. Kuznetsov,^{ae} and Andrei V. Shevelkov*^a

^a Department of Chemistry, Lomonosov Moscow State University, Moscow 119991, Russia. E-mail: shev@inorg.chem.msu.ru

^b National Institute for Chemical Physics and Biophysics, 12618 Tallinn, Estonia.

^c Department of Physics, Lomonosov Moscow State University, Moscow 119991, Russia.

^d P. N. Lebedev Physics Institute RAS, Moscow 119991, Russia.

^e N. S. Kurnakov Institute of General and Inorganic Chemistry RAS, Moscow 119991, Russia

Table of contents

1. Experimental Procedures S1
2. Results and discussion S3
3. References S6

1. Experimental Procedures

1.1. Synthesis. Synthesis of a polycrystalline sample of ReGaGe₂ was carried out by the standard ampule technique in two steps. First, Re powder (99.99%, Sigma-Aldrich), Ge chips (99.999%, Sigma-Aldrich) and Ga (99.9999%, Sigma-Aldrich) used as starting materials were mixed in a stoichiometric ratio and placed inside a quartz ampule, which was evacuated to the residual pressure of 1×10^{-3} Torr and sealed. The sample was annealed at 950°C for 2 days to ensure the complete reaction of the elements, and then the temperature was reduced to 750°C and remained for 5 days. After the first annealing, the sample was ground, pressed into pellets, and annealed at 750°C for 7 days in evacuated quartz ampule. After the second annealing and regrinding, a black, air- and moisture-stable, homogeneous powder was obtained.

1.2. Crystal structure determination. Crystal structure was investigated by X-ray powder diffraction (Fig. S1) using Cu K α 1, 2 radiation (BRUKER D8 Advance diffractometer, $\lambda = 1.540593, 1.544427 \text{ \AA}$). The unit cell parameters were calculated using the standard program package StoeWinXPOW v.1.06. The crystal structure of the new compound was determined using the Space group test and Superflip options implemented in the Jana2006 package.¹ Upon determining the crystal structure, all *p*-element positions were set as occupied by gallium and germanium according to the nominal composition. The crystallographic data, refinement details, and atomic parameters are presented in Table S1 and Table S2. CCDC 1896999 contains the supplementary crystallographic data for this paper. These data are provided free of charge by The Cambridge Crystallographic Data Centre.

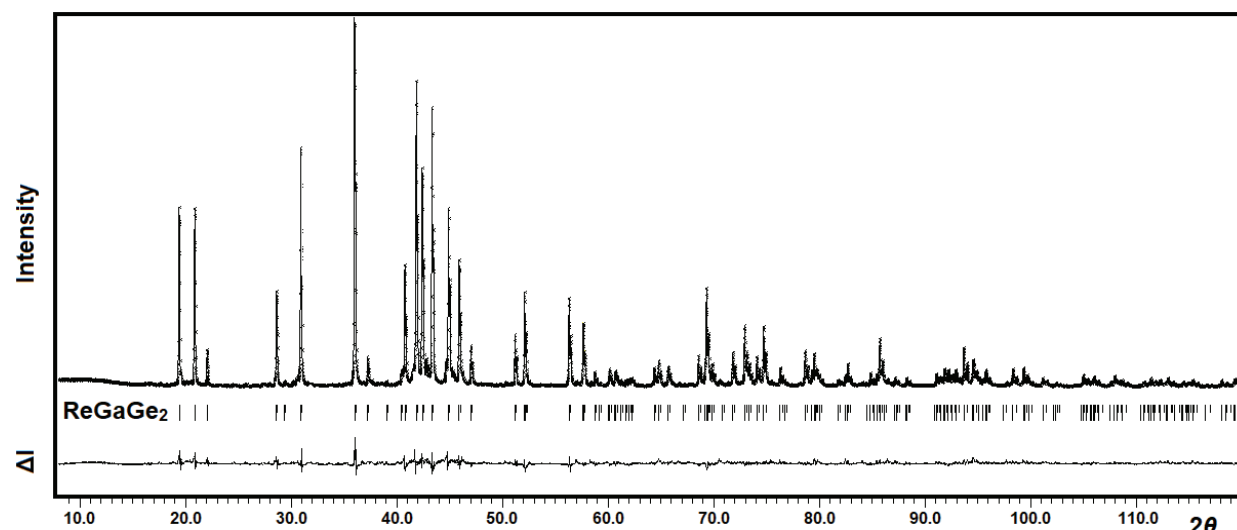


Fig. S1. Powder X-ray diffraction pattern for ReGaGe₂.

Table S1. Crystallographic and Refinement Parameters for ReGaGe₂ at 293K

| formula | ReGaGe ₂ | |
|---|---------------------|-----------------------|
| formula (g·mol ⁻¹) | weight | 401.1 |
| Crystal system | | orthorhombic |
| Space group | | Cmcm |
| a (Å) | | 3.26861(4) |
| b (Å) | | 9.17461(12) |
| c (Å) | | 8.53206(10) |
| V (Å ³) | | 255.861(5) |
| Z | | 4 |
| ρ _{calc} (g·cm ⁻³) | | 10.413 |
| temperature (K) | | 293 |
| radiation, λ (Å) | Cu Kα, | 1.540593, 1.544427 |
| 2θ range (deg) | | 8.00 – 120.0 |
| R ₁ | | 0.0539 |
| wR ₂ | | 0.0678 |
| GoF | | 1.63 |

Table S2. Atomic coordinates and thermal displacement parameters for the ReGaGe₂

| atom | Wyckoff position | x | y | z | U _{ani} , Å ² | occupancy |
|------|------------------|---|-----------|-----------|-----------------------------------|--------------|
| Re1 | 4c | 0 | 0.7216(1) | 1/4 | 0.0291(4) | 1 |
| E1 | 8f | 0 | 0.1349(2) | 0.0327(2) | 0.0344(8) | 1/3Ga+2/3Ge* |
| E2 | 4c | 0 | 0.4431(3) | 1/4 | 0.0366(11) | 1/3Ga+2/3Ge* |

* - fixed according to the composition

1.3. EDXs analysis. For determination of the chemical composition, the as-prepared sample of ReGaGe₂ was finely ground and pressed into a pellet. Investigation was carried out using a scanning electron microscope JSM JEOL 6490-LV equipped with an energy dispersive X-ray (EDX) analysis system INCA x-Sight.

1.4. NQR spectroscopy. The ^{69,71}Ga NMR/NQR measurements were performed at 4.2 K utilizing a home-built phase coherent pulsed NMR/NQR spectrometer with direct digital quadrature detection at the carrier frequency. The ^{69,71}Ga NQR spectra were measured using a frequency step point-by-point spin-echo technique. At each frequency point, the area under the spin-echo magnitude was integrated in the time domain and averaged by a number of accumulations, which depends on the Ga isotope and frequency. Alternatively, we used a Fourier transform summation method for broad spectra accumulation.²

1.5. Computational details. Electronic structure calculations were performed on the Density Functional Theory (DFT) level using two approaches: i) an all-electron full-potential linearized augmented plane wave method (FP-LAPW) as implemented in the ELK code,³ and ii) a pseudopotential projector augmented wave method (PAW) as implemented in the Vienna *ab initio* Simulation Package (VASP).⁴ In the first approach, PBESol⁵, WC06⁶ exchange-correlation functional of the GGA-type, and SCAN⁷ functional of metaGGA type were utilized. For the PBESol computations, we performed energy calculations with spin-orbit coupling switched off and on. The Brillouin zone sampling was performed using a 16×11×6 *k*-point grid (530 irreducible *k*-points), the muffin-tin sphere radii for the respective atoms were (Bohr): 2.46 (Re), 2.29 (Ga), 2.29 (Ge), and the maximum moduli for the reciprocal vectors *k*_{max} were chosen such that *R_{MT}k*_{max}= 10.0. In the second, pseudopotential approach, a Monckhorst-Pack *k*-point mesh⁸ of 14×6×6 (63 irreducible *k*-points) was employed, and the energy cutoff was set at 500 eV. The PBE⁹, PBESol, and SCAN exchange-correlation functionals were used in the PAW-based calculations. The convergence of the total energy with respect to the *k*-point sets was checked.

Unit cell parameters and atomic coordinates from the experiment were taken as starting points for calculations. In both FP-LAPW and PAW approaches, we considered two models: 1) the fully ordered one where all the Ge atoms were occupying the 8f position (E1), and all the Ga ones – 4c (E2), which directly reflects the stoichiometry, and 2) the one with two Ga atoms are swapped with two Ge ones, which represents partial disorder. The third model, representing complete statistical disorder of the original unit cell through the Virtual Crystal Approximation (VCA), was used exclusively in the FP-LAPW calculations. For that purpose, a fractional atom simulating 66.7% Ge and 33.3% Ga occupancy of the same atomic position was created using the internal routine of the ELK program and used to represent the *p*-block elements in the structure. For the energy comparisons between first two

models, we have also performed atomic coordinate relaxation within fixed unit cells, using ELK package and PBESol functional. In order to allow atoms to shift from their positions, all symmetry elements were removed and the structures were represented by P1 space group.

Atomic charges were calculated according to Bader's quantum theory of atoms in molecules (QTAIM).¹⁰ The electron localizability indicator (ELI-D) was calculated according to the literature¹¹ using DGrid package.¹² Structure visualization and topological analysis of the electron localization indicator were performed using VESTA 3.4.4¹³ and ParaView 5.2.0¹⁴ packages, respectively. The results of the VASP calculations were visualized using wxDragon package.¹⁵

1.6. Transport properties investigation. For resistivity, Seebeck coefficient, and thermal conductivity measurements, dense pellets were prepared by spark plasma sintering (SPS) using a Labox-625 machine. Densification was performed in 10 mm graphite dies by heating the sample to 973 K at 70 K/min under a pressure of 60 MPa in vacuum, keeping it at this temperature for 7 min, and then cooling down to room temperature. The relative density of the sample of approximately 92% (geometrical) or 90% (Archimedean) was achieved. The purity of the sample after SPS pressing was controlled by XRD analysis, which showed no changes after the experiment. Electrical resistivity, Seebeck coefficient and thermal conductivity were measured on a parallelepiped-shaped sample, cut from the pellet obtained by SPS, with a dimension of $8 \times 3 \times 2$ mm³ using resistivity and thermal transport options of the Physical Property Measurement System (PPMS, Quantum Design), respectively, in the temperature range of 2 – 400 K. All measurements were carried out in zero magnetic field.

2. Results and Discussion

2.1. Elemental analysis. EDXs analysis demonstrates full agreement of the measured composition with the nominal one (see Table S3).

Table S3. Determined and nominal composition of the ReGaGe₂

| | Re, at. % | Ga, at. % | Ge, at. % | composition |
|----------|-----------|-----------|-----------|---|
| Nominal | 25 | 25 | 50 | ReGaGe ₂ |
| Measured | 24.8(3) | 25.3(4) | 49.9(3) | Re _{0.99(1)} Ga _{1.01(2)} Ge _{2.00(1)} |

2.2. NQR spectroscopy

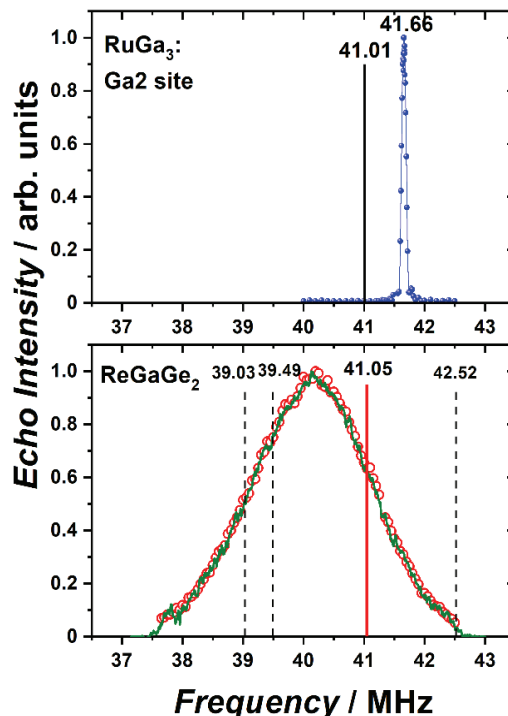


Fig. S2. ⁶⁹Ga NQR spectra of ReGaGe₂ (bottom panel) and RuGa₃ at Ga2 site (top panel) measured at 4.2 K. Circles correspond to spin-echo integration method; green solid line – Fourier transform summation. Vertical solid lines indicate ⁶⁹Ga quadrupole frequencies calculated for stoichiometric Ga positions in these compounds using VASP program. Dashed lines (bottom panel) indicate Ga frequencies for the simplest case of one Ge atom substituted for Ga in the 1st coordination sphere of Ga nuclei.

2.3. On the compliance with the 18-n rule. The rhenium-rhenium distance in ReGaGe₂ is 3.269 Å, which is greater than the distance in metallic Re (2.74–2.77 Å). Apparently, such a distance can not be considered as an actual covalent bond between the

rhenium atoms, but it might be considered an isolobal bond according to the $18 - n$ formalism. Since the Re atoms form a chain along the a axis the value of n is 2 (Fig. 1b in the main text). Moreover, there is one orthogonal E–E bond between E1 atoms of 2.537\AA per each Re atom, therefore the value of m is 2 (Fig. 1c in the main text). Thus, the valence electrons concentration ($18 = 7(\text{Re}) + 3(\text{Ga}) + 4 \times 2 (\text{Ge})$) corresponds to the $18 - n + m$ rule, where $n = 2$ and $m = 2$, and also predicts semiconducting behavior of ReGaGe_2 .

2.4. Electronic structure calculations. Since both initial calculations and physical measurements indicated semiconducting behavior of ReGaGe_2 , we deemed it important to study the dependence of calculated band gap on the computational conditions. In order to estimate the performance of the DFT methods, we used both FP-LAPW and PAW approaches and employed several well-established exchange-correlation functionals of the GGA-type, such as Perdew-Burke-Ernzerhof (PBE), Perdew-Burke-Ernzerhof revised for solids (PBESol), Wu-Cohen 06 (WC06), as well as recently introduced Strongly Constrained and Appropriately Normed Semilocal Density Functional (SCAN) of the meta-GGA type. We have also investigated the effect of spin-orbit coupling (SOC) upon the band gap value, since for such heavy element as rhenium it might be a factor influencing band structure near the Fermi level. All the calculations were performed for two ordered models. In the first one, which we call fully ordered, the E1 position is fully occupied by germanium, and the E2 position is fully occupied by gallium, which gives the exact stoichiometry of ReGaGe_2 . In the second one, we swap gallium atoms in the E2 position and part of germanium atoms in the E1 position, which we call partially disordered model because here we have heteroatomic Ga-Ge dumbbells. The third case we consider is full statistical disorder, which we model using Virtual Crystal Approximation (VCA), only implemented in the FP-LAPW package. For that purpose a pseudoatom with a number of electrons of 31.67 was created and put into both E1 and E2 positions, which simulates the occupancy of each E position with $1/3$ Ga and $2/3$ Ge. The results are summarized in Fig. S3 and Table S3. The difference between fully ordered and partially disordered models is minimal, so we only show results for fully ordered and VCA models.

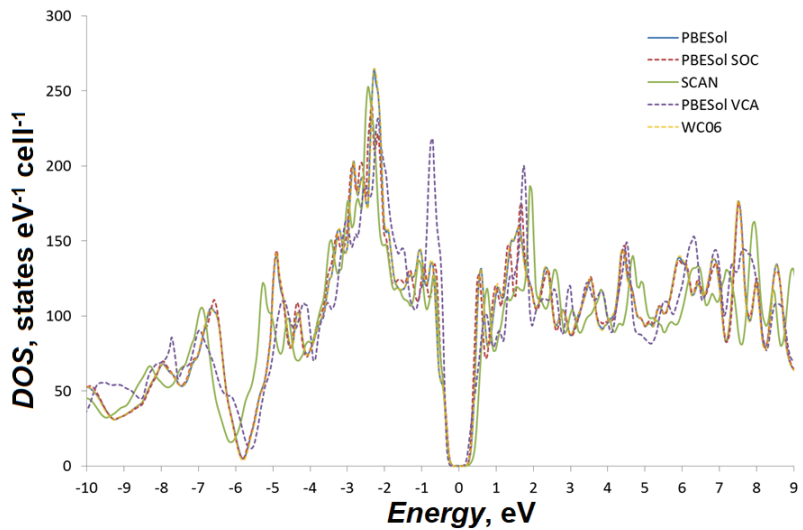


Fig. S3. Calculated TDOS for ReGaGe_2 from different computational DFT-based approaches.

Table S4. Calculated band gaps for ReGaGe_2 from different computational conditions

| Computational conditions | FP ^[a] / PBESol | PAW ^[b] / PBESol | PAW ^[b] / PBE | FP ^[a] / WC06 | FP ^[a] / SCAN | FP ^[a] / PBESol / VCA | FP ^[a] / PBESol / SOC |
|--------------------------|----------------------------|-----------------------------|--------------------------|--------------------------|--------------------------|----------------------------------|----------------------------------|
| Band gap, eV | 0.42 | 0.42 | 0.39 | 0.42 | 0.45 | 0.38 | 0.43 |

(a)all-electron full-potential linearized augmented plane-wave approach. (b) pseudopotential projector augmented wave approach.

As seen from both Fig. S3 and Table S4, the results from all the approaches are in good agreement, with no outliers and all band gap values falling into the 0.38–0.45 eV range. This in itself does not mean that the real band gap cannot be underestimated in our calculations (as often happens with DFT calculations on semiconductors), but the consistency of the results and the use of advanced meta-GGA SCAN functional indicate that we are most likely not far off the real gap value. And although it was not our goal here to calculate band gap exactly, but rather to be certain to avoid unexpected computational errors, based on the results we can state with high degree of certainty that ReGaGe_2 is a narrow-gap semiconductor with band gap ca. 0.4 – 0.45 eV. Notably, fully ordered and fully disordered (VCA) models have calculated band gaps within 0.04 eV, i.e. these extreme cases are not dramatically different electronic structure-wise. Also, we observe that spin-orbit coupling does not affect the density of

states and band structure near the Fermi level in a serious way, which might be partially attributed to both the nature of valence electrons of rhenium and its relatively low content in the unit cell.

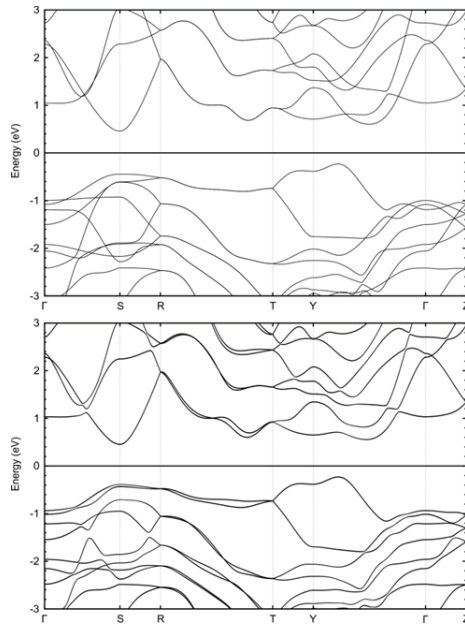


Fig. S4. Calculated band dispersion near the Fermi level for ReGaGe_2 : ordered model, PBESol functional, top – without spin-orbit coupling, bottom – with spin-orbit coupling taken into account (For the explanation see the text).

2.5. ELI-D topological analysis. As seen from Fig. S5, at higher γ values ($\gamma=1.25$) the first features to appear are E-E pairwise interactions (shown as dark blue pucks). In the ordered model these are Ge-Ge dumbbells, but since the electronic structure does not change in a significant way when completely disordered Ga/Ge distribution is modeled, the presence of Ga-Ge heteroatomic units would have the same features. Next, as we go down to $\gamma=1.15$, we start to observe pairwise Re-E interactions, in the ordered model – Re-Ge. At $\gamma=1.07$ we observe Re-Ga bonds, also as a pairwise interactions. No further attractors appear upon lowering the γ value from that point. Also, no attractors are observed that would correspond to direct Re-Re bonds (as illustrated by ELI-D isosurface at $\gamma=1.10$). Thus, there are two distinct pairwise interactions upon which the structure is built – E-E and Re-E covalent bonds.

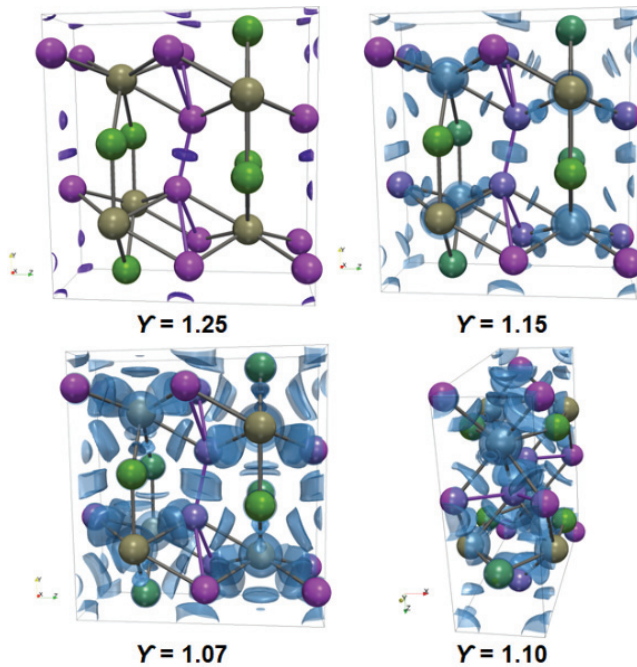


Fig. S5. ELI-D topology for ReGaGe_2 .

3. References

1. V. Petricek, M. Dusek, L. Palatinus, *Z. Kristallogr. – Cryst. Mater.* 2014, **229**(5), 345–352.
2. W. G. Clark, M. E. Hanson, F. Lefloch, P. Ségransan, *Rev. Sci. Instrum.* 1995, **66**, 2453.
3. ELK, an all-electron full-potential linearised augmented-plane wave (FP-LAPW) code, ver. 3.1.12; <http://elk.sourceforge.net>
4. a) G. Kresse, D. Joubert, *Phys. Rev. B* 1999, **59**, 1758–1775. b) G. Kresse, J. Furthmüller, *Vienna Ab-initio Simulation Package (VASP)*, v.5.4.4; <http://vasp.at>
5. J. P. Perdew, A. Ruzsinszky, G. I. Csonka, O. A. Vydrov, G. E. Scuseria, L. A. Constantin, X. Zhou, K. Burke, *Phys. Rev. Lett.* 2008, **100**, 136406.
6. Z. Wu, R. E. Cohen, *Phys. Rev. B* 2006, **73**, 235116.
7. J. Sun, A. Ruzsinszky, J. P. Perdew, *Phys. Rev. Lett.* 2015, **115**, 036402.
8. H. J. Monckhorst, J. D. Pack, *Phys. Rev. B* 1976, **13**, 5188–5192.
9. J. P. Perdew, K. Burke, M. Ernzerhof, *Phys. Rev. Lett.* 1996, **77**, 3865.
10. R. F. W. Bader, *Atoms in Molecules: A Quantum Theory*; Oxford University Press, Oxford, U.K., 1990.
11. a) M. Kohout, *Int. J. Quantum Chem.* 2004, **97**, 651–658. b) M. Kohout, *Faraday Discuss.* 2007, **135**, 43–54. c) M. Kohout, K. Pernal, F. R. Wagner, Yu. Grin, *Theor. Chem. Acc.* 2004, **112**, 453–459.
12. M. Kohout. *DGrid*, ver. 4.6; Radebeul, 2011.
13. K. Momma, F. Izumi, *J. Appl. Crystallogr.* 2011, **44**, 1272–1276.
14. ParaView ver. 5.2.0, Open Source Scientific Visualization; www.paraview.org
15. wxDragon 2.1.6; <http://www.wxdragon.de>